Mineralogical Magazine, February 2009, Vol. 73(1), pp. 131–148

Description and crystal structure of a new mineral – plimerite, $ZnFe_4^{3+}(PO_4)_3(OH)_5$ – the Zn-analogue of rockbridgeite and frondelite, from Broken Hill, New South Wales, Australia

P. Elliott[1,5], U. Kolitsch[2], G. Giester[3], E. Libowitzky[3], C. McCammon[4], A. Pring[5], W. D. Birch[6] and J. Brugger[1,5]

[1] School of Earth and Environmental Sciences, The University of Adelaide, Adelaide, South Australia 5005, Australia
[2] Mineralogisch-Petrographische Abt., Naturhistorisches Museum, A-1010 Wien, Austria
[3] Institut für Mineralogie und Kristallographie, Geozentrum, Universität Wien, Althanstrasse 14, A-1090 Wien, Austria
[4] Bayerisches Geoinstitut, Universität Bayreuth, D-95440 Bayreuth, Germany
[5] South Australian Museum, North Terrace, Adelaide, South Australia 5000, Australia
[6] Geosciences, Museum Victoria, GPO Box 666, Melbourne 3001, Victoria, Australia

[*Received 5 January 2009; Accepted 5 April 2009*]

ABSTRACT

Plimerite, ideally $ZnFe_4^{3+}(PO_4)_3(OH)_5$, is a new mineral from the Block 14 Opencut, Broken Hill, New South Wales. It occurs as pale-green to dark-olive-green, almost black, acicular to prismatic and bladed crystals up to 0.5 mm long and as hemispherical aggregates of radiating acicular crystals up to 3 mm across. Crystals are elongated along [001] and the principal form observed is {100} with minor {010} and {001}. The mineral is associated with hinsdalite-plumbogummite, pyromorphite, libethenite, brochantite, malachite, tsumebite and strengite. Plimerite is translucent with a pale-greyish-green streak and a vitreous lustre. It shows an excellent cleavage parallel to {100} and {010} and distinct cleavage parallel to {001}. It is brittle, has an uneven fracture, a Mohs' hardness of 3.5–4, D(meas.) = 3.67(5) g/cm^3 and D(calc.) = 3.62 g/cm^3 (for the empirical formula). Optically, it is biaxial negative with α = 1.756(5), β = 1.764(4), γ = 1.767(4) and $2V$(calc.) of −63º; pleochroism is X pale-greenish-brown, Y pale-brown, Z pale-bluish-green; absorption Z > X > Y; optical orientation XYZ = *cab*. Plimerite is orthorhombic, space group *Bbmm*, unit-cell parameters: a = 13.865(3) Å, b = 16.798(3) Å, c = 5.151(10) Å, V = 1187.0(4) Å^3 (single-crystal data) and Z = 4. Strongest lines in the X-ray powder diffraction pattern are [d (Å), I, hkl]: 4.638, (50), (111); 3.388, (50), (041); 3.369, (55), (131); 3.168, (100), (132); 2.753, (60), (115); 2.575, (90), (200); 2.414, (75), (220); 2.400, (50), (221); 1.957, (40), (225). Electron microprobe analysis yielded (wt.%): PbO 0.36, CaO 0.17, ZnO 20.17, MnO 0.02, Fe_2O_3 29.82, FeO 2.98, Al_2O_3 4.48, P_2O_5 32.37, As_2O_5 0.09, H_2O (calc) 6.84, total 97.30 (Fe^{3+}/Fe^{2+} ratio determined by Mössbauer spectroscopy). The empirical formula calculated on the basis of 17 oxygens is $Ca_{0.02}Pb_{0.01}Zn_{1.68}Fe^{2+}_{0.28}Fe^{3+}_{2.53}Al_{0.60}P_{3.09}As_{0.01}O_{17.00}H_{5.15}$. The crystal structure was solved by direct methods and refined to an $R1$ index of 6.41% for 1332 observed reflections from single-crystal X-ray diffraction data (Mo-$K\alpha$ radiation, CCD area detector). The structure of plimerite is isotypic with that of rockbridgeite and is based on face-sharing trimers of ($M\phi_6$) octahedra which link by sharing edges to form chains, that extend in the b-direction. Chains link to clusters comprising pairs of corner-sharing ($M\phi_6$) octahedra that link to PO_4 tetrahedra forming sheets parallel to (001). The sheets link *via* octahedra and tetrahedra corners into a heteropolyhedral framework structure. The mineral name honours Professor Ian Plimer for his contributions to the study of the geology of ore deposits.

* E-mail: peter.elliott@adelaide.edu.au
DOI: 10.1180/minmag.2009.073.1.131

Keywords: plimerite, rockbridgeite, frondelite, new mineral species, Zn-Fe phosphate, crystal structure, Broken Hill, New South Wales, Australia.

Introduction

The Broken Hill Pb-Zn-Ag deposit in western New South Wales is the largest Pb-Zn orebody in the world, and has been mined continuously since its discovery in 1883, producing 200 Mt of ore. From 1984 until the late 1990s, mining of remnant-oxidized ore on the old South Mine leases resulted in the addition of some 70 species to the list of recorded minerals from Broken Hill and also in a much-improved knowledge of the secondary mineral assemblages and their distribution in the oxidized zone (Birch and van der Heyden, 1988; Birch, 1990; Birch and van der Heyden, 1997).

Rockbridgeite was one of several Fe phosphates identified during this phase of mining. A Zn-rich rockbridgeite, with up to 30% of Fe being replaced by Zn, was recognized as a probable new mineral species in the mid 1980s (Birch, 1990), but as single crystals suitable for structure determination could not be located, the extent of ordering of Fe and Zn between cation sites in the rockbridgeite structure was not known. As a result, efforts to characterize fully the mineral as a new phase were not successful.

In the late 1990s, specimens with larger and better-quality crystals than any previously found were collected from ore mined from the Block 14 Opencut. Some crystals have proved suitable for collection of single-crystal X-ray data and have allowed a more complete characterization of the mineral.

The mineral and its name have been approved by the IMA Commission on New Minerals, Nomenclature and Classification (IMA 2008-013). The mineral is named for Professor Ian Plimer, Professor of Mining Geology, The University of Adelaide and Emeritus Professor of Earth Sciences, The University of Melbourne, in recognition of his contributions to the geology of ore deposits, and in particular the geology of the Broken Hill deposit, and also his service to a number of professional organizations. Type material is preserved in the Department of Mineralogy of the South Australian Museum, Adelaide, South Australia (Registration number G32005).

Plimerite is the Zn analogue of rockbridgeite, $Fe^{2+}Fe^{3+}_4(PO_4)_3(OH)_5$, and frondelite, $Mn^{2+}Fe^{3+}_4(PO_4)_3(OH)_5$ (Table 1), minerals which are widespread as typical alteration products of primary phosphates in granite pegmatites, also found in Fe-ore deposits, sedimentary phosphate deposits and greisens.

Research into the basic transition metal phosphates, in particular those of Fe^{2+}, Fe^{3+}, Mn^{2+} and Mn^{3+}, such as barbosalite, cacoxenite, dufrénite, frondelite, rockbridgeite, beraunite, souzalite, tinticite and 'laubmannite', has been challenging mineralogists since dufrénite was first discovered in the early 1800s (Frondel, 1949; Moore, 1969; Moore, 1970). Many have remained poorly characterized since their discovery. Frondel (1949) observed that the identity of several of the basic Fe phosphates had been confused since earliest times under the name dufrénite (e.g. Massie, 1880, Campbell, 1881). The minerals frequently have very similar chemical compositions and can have similar appearance, and physical and optical properties can vary widely within a single species and are often similar to those of other species. Many species have variable water content and non-essential impurities and they also produce poor quality X-ray powder diffraction patterns. Frondel (1949) provided a review of the history and nomenclature of these minerals. He found that, although indistinguishable from dufrénite in general appearance, about half of the specimens labelled 'dufrénite' examined in the course of his study gave an X-ray powder pattern distinct from that of dufrénite. Frondel recorded nine occurrences for the most common of these distinct species, and named the mineral rockbridgeite after the occurrence near Midvale, Rockbridge County, Virginia. The formula of rockbridgeite was given by Frondel (1949) as most likely to be $Fe^{2+}Fe^{3+}_6(PO_4)_4(OH)_8$ based on four analyses. Lindberg (1949) gave the formula as $Fe^{2+}Fe^{3+}_4(PO_4)_3(OH)_5$ based on two analyses, and this formula was confirmed by the crystal-structure analysis of Moore (1970). Frondelite, $Mn^{2+}Fe^{3+}_4(PO_4)_3(OH)_5$, was described by Lindberg (1949) from the Sapucaia pegmatite, Minas Gerais, Brazil.

The general formula of rockbridgeite-frondelite is $AB_4(PO_4)_3(OH)_5$, with the *A* site occupied by divalent cations (Fe^{2+} and Mn^{2+}) and the *B* site occupied by trivalent cations (Fe^{3+}). Analyses have shown compositions ranging from the pure Fe^{2+} and Mn^{2+} end members to intermediate

TABLE 1. Comparison of plimerite, rockbridgeite and frondelite.

	Plimerite	Rockbridgeite	Frondelite
Locality	Broken Hill, NSW, Australia	Irish Creek, VA., USA	Sapucaia pegmatite, Minas Gerais, Brazil
Reference	this work	Frondel (1949), Moore (1970)	Lindberg (1949)
Formula	$Zn(Fe^{3+},Zn,Al)_4(PO_4)_3(OH)_5$	$Fe^{2+}Fe_4^{3+}(PO_4)_3(OH)_5$	$(Mn^{2+}Fe^{2+})Fe_4^{3+}(PO_4)_3(OH)_5$
Symmetry	orthorhombic	orthorhombic	orthorhombic
Space group	*Bbmm*	*Bbmm*	*Bbmm*
a (Å)	13.811(3)	13.783(12)	13.81
b (Å)	16.718(3)	16.805(9)	16.968
c (Å)	5.141(10)	5.172(4)	5.182
V (Å^3)	1187.07(7)	1197.96	1214.29
Z	4	4	4
Strongest lines in the X-ray powder pattern	4.638(50), 3.388(50), 3.369(55), 3.168(100), 2.753(60), 2.575(100), 2.414(75), 2.400(50), 1.957(40)	6.87(4), 4.842(5), 4.630(4), 3.573(5), 3.433(4), 3.364(4) 3.196(10), 2.754(4), 2.409(5), 2.052(4), 1.833(4), 1.589(5)	3.191 (100), 3.381 (85), 3.615 (40), 3.445 (25), 3.046 (20), 1.5953 (19), 6.91 (17)
$D_{meas.}$; $D_{calc.}$	3.67; 3.62	3.45, 3.60	3.453; 3.35
Mohs hardness	3.5-4	3.5-4.5	4.5
α	1.756(5)	1.873	1.86
β	1.764(4)	1.880	1.88
γ	1.767(4)	1.895	1.893
Birefringence	0.011	0.022	0.033
Opt. character	biaxial negative	biaxial positive	biaxial negative
2V (meas.); (calc.)	large; 63º	moderate (meas.)	moderate (meas.)
Dispersion	present, but character unknown	r > v	r > v
Orientation	XYZ = *cab*		X = *c*
Elongation	negative (length-fast)		
X (colour)	pale greenish-brown	pale brown to pale yellow	pale yellow-brown
Y (colour)	pale brown	bluish-green	orange-brown
Z (colour)	(pale) bluish-green	dark bluish-green	orange-brown
Absorption	Z >X> Y	Z>Y>X	Z>Y>X
Megascopic colour	pale olive-green to greenish-black	greenish-black	dark brown, ochre-yellow, red-brown, orange, greenish-brown
Streak	pale greyish-green	greenish-grey	brownish-grey
Habit	bladed, prismatic, acicular, elongated along [001], radiating sprays, hemispherical aggregates	euhedral crystals rare, fibrous, elongated along [001], compact radiating, crusts, botryoidal and drusy masses.	euhedral crystals rare, fibrous, elongated along [001], radiating, crusts, botryoidal, drusy masses.
Twinning	none observed	none observed	none observed
Cleavage	{100}, good; {010}, good; {001}, distinct	{100}, excellent; {010}, good; {001}, fair	{100}, excellent; {010}, good; {001}, fair
Fracture	uneven	uneven	uneven

compositions [e.g. from the Fletcher Mine, New Hampshire, USA (Frondel, 1949); the Palermo Mine, New Hampshire, USA (analysis of Gonyer, cited by Frondel, 1949), Polk County, Arkansas, USA (analysis of Hallowell, cited by Frondel, 1949)].

Zincian rockbridgeite has been reported from several localities. Black crusts and small botryoidal masses with a radial fibrous or thin-bladed structure were found in a pegmatite at Vianua do Castelo, Maxedo, Portugal (Lindberg and Frondel, 1950). The zincian rockbridgeite, which contains up to 5.20 wt.% ZnO, was formed by the hydrothermal alteration of triphylite containing admixed sphalerite. The authors considered Zn^{2+} to occupy the *B* site in the

general formula, but their reasoning for this is not clear.

Minerals of the rockbridgeite–frondelite series occur in a complex assemblage of phosphate minerals in the Huber Shaft, Krásno district, Czech Republic (Sejkora *et al*., 2006*a*). The mineralization is associated with quartz in greisens and was derived from primary triplite and fluorapatite. Analyses of many samples have shown compositions between end members frondelite and rockbridgeite with up to 0.65 a.p.f.u. (atoms per formula unit) Fe^{2+}. Some however have compositions with up to 19.19 wt.% ZnO (Sejkora *et al*., 2006*b*), which would fall into the compositional range of plimerite.

Zincian rockbridgeite has also been reported by Ginzburg (1952) from granite pegmatites in Turkestan and the Kalbin Range (Central Asia) associated with Fe-, Mn- and Al phosphates, and an unidentified Zn phosphate from the Sapucaia pegmatite, Minas Gerais, Brazil mentioned by Hirson (1965) is most likely a zincian rockbridgeite.

The present study has confirmed, by X-ray diffraction (XRD) and electron microprobe analysis (Table 2), that rockbridgeite from Reaphook Hill, Flinders Range, South Australia (Johnson, 1978) is plimerite.

Based on single-crystal rotation and Weissenberg photographs using a cleavage fragment, Lindberg (1949) tentatively assigned space groups $B22_1$ or $B22_12$ for frondelite, and from powder X-ray photographs gave unit-cell parameters of a = 13.89 Å, b = 17.01 Å, c = 5.27 Å, V = 1245.12 Å^3 for frondelite, and a = 13.76 Å, b = 16.94 Å, c = 5.19 Å, V = 1209.76 Å^3 for rockbridgeite.

The structure of rockbridgeite was first described by Moore (1970), using long-exposure Weissenberg photographs and visual intensity estimations. Moore deduced space group *Bbmm* (a non-standard setting of *Cmcm*) and gave unit-cell parameters a = 13.783(12) Å, b = 16.805(9) Å, c = 5.172(4) Å, V = 1197.96 Å^3. The structure solution was, however, not ideal, with some isotropic atomic-displacement parameters having negative values, so an anisotropic model was not completed. The structure has three Fe sites, and based on average Fe–O distances [Fe(1)–O = 2.07; Fe(2)–O = 2.11; Fe(3)–O = 2.00 Å], Moore (1970) assigned a mixture of Fe^{2+} and Fe^{3+} to the Fe(1) and Fe(2) sites in the structure, and Fe^{3+} to the Fe(3) site. However, the relatively high

TABLE 2. Electron microprobe analyses in wt.%.

Sample	Broken Hill (G32005)	Broken Hill (G32402)	Broken Hill (G32401)	Reaphook Hill
P_2O_5	32.37	33.98	33.13	30.92
As_2O_5	0.09	0.05	0.23	0.04
Al_2O_3	4.48	1.89	0.93	1.48
Fe_2O_3	29.82	31.62	36.42	33.51
FeO	2.98	3.52	4.47	3.73
MnO	0.02	0.36	0.04	0.56
MgO	0.00	0.11	0.00	0.84
CaO	0.17	0.80	0.14	1.41
CuO	0.00	0.00	0.24	0.00
ZnO	20.17	18.52	14.43	18.38
PbO	0.36	0.20	0.37	0.03
H_2O (calc)*	6.84	6.84	6.84	6.84
Total	97.30	97.89	97.24	97.74

The empirical formulae of two of the analyses above are:
(G32005): $Ca_{0.02}Pb_{0.01}Zn_{1.68}Fe^{2+}_{0.28}Fe^{3+}_{2.53}Al_{0.60}As_{0.01}P_{3.09}O_{17.00}H_{5.15}$;
(G32401): $Ca_{0.02}Pb_{0.01}Zn_{1.20}Fe^{2+}_{0.42}Fe^{3+}_{3.09}Al_{0.12}As_{0.01}P_{3.16}O_{17.00}H_{5.14}$

Formulae are based on 17 oxygen atoms.

* calculated from structure solution.

estimated standard uncertainties left these assignments in some doubt.

More recently, a reinvestigation of the rockbridgeite structure, using a specimen of manganoan rockbridgeite from the Hagendorf pegmatite, Bavaria, Germany, made use of single-crystal X-ray and ^{57}Fe Mössbauer data and specifically investigated the cation distribution in the structure (Redhammer *et al*., 2006). The occupancy of the Fe(1) and Fe(3) sites in the structure by Fe^{3+}, and the occupancy of the Fe(2) site, principally by Fe^{2+}, was confirmed. The 0.62 a.p.f.u. Mn in the formula, partially occupying the Fe(2) site, was considered by the authors to be trivalent on the basis of the Jahn-Teller distortion of the Fe(2) site.

The crystal structure of frondelite is not known at present.

Occurrence

The Broken Hill deposit comprises a number of discrete masses of high- to low-grade sulphide rocks of varying chemistry and mineralogy within highly deformed siliclastic metasedimentary rocks of the Palaeoproterozoic Willyama Supergroup. The region has undergone multiphase metamorphism and deformation to granulite and upper amphibolite facies (Willis *et al*., 1983). A long and complex history of weathering has resulted in an extensive oxidized zone, which reaches a maximum depth of 100 m and is notable for the complexity of its mineralogy (Birch, 1999).

During mining in the mid- to late-1980s, phosphate-rich zones with a diverse range of Pb, Fe, Zn and Cu phosphate minerals were exposed in the No. 3 Lens of the Block 14 Opencut and at the 310 m level in the B lode of the Kintore Opencut (Birch and van der Heyden, 1997). The phosphate suites are presumably derived from weathering of primary fluorapatite, which is a common accessory mineral in the sulphide orebody.

Rockbridgeite was one of several Fe-bearing phosphate minerals identified, along with beraunite, chalcosiderite, cyrilovite, dufrénite-natrodufrénite, kidwellite, leucophosphite and strengite, and was relatively common in the phosphate zone in the Block 14 Opencut. The rockbridgeite forms sprays and globular crusts of tiny (<0.1 mm) olive- to dark-greyish-green crystals from the Kintore Opencut and lustrous globules to 1 mm and fibrous grey-green crusts grading into distinct grey-green blocky crystals up to 0.2 mm associated with corkite, libethenite and tsumebite from the 275 m level of the Block 14 Opencut.

Constructing a simple paragenetic model for the oxidized zone has presented difficulties due to the number of variables involved. Documentation of material from the Kintore and Block 14 Opencuts identified three or four broad associations, which could be spatially related (Birch and van der Heyden, 1988). These were (1) a series rich in Zn; (2) an arsenate-rich assemblage; (3) an Fe- and phosphate-rich assemblage; (4) a suite of Zn and Cu sulphates. The following paragenesis for the suite of secondary phosphate minerals was proposed by Birch (1990):

corkite–hinsdalite → turquoise–chalcosiderite → leucophosphite → dufrénite/rockbridgeite → kidwellite → beraunite → sampleite/strengite → torbernite

Plimerite-zincian rockbridgeite is found in seams and cavities in quartz-garnet-goethite-rich rocks from the Block 14 Opencut. On the type specimen, plimerite is associated with crusts of white to yellow hinsdalite-plumbogummite, white prisms of calcian pyromorphite, sprays of pale-green libethenite prisms, greenish-blue brochantite crystals and aggregates of acicular malachite crystals. On other specimens, additional associated minerals are greenish-blue crystals of tsumebite and hemispherical aggregates of pinkish-white strengite crystals.

At Reaphook Hill, plimerite occurs as green- to greenish-yellow crystal aggregates and druses, and is associated with scholzite, parahopeite, collinsite–hillite and eosphorite (containing ~2.1 wt.% ZnO according to EPMA data).

Appearance, physical and optical properties

Plimerite occurs as pale-green to dark-olive-green hemispherical aggregates of radiating acicular crystals and less commonly as pale-olive-green to dark-green, almost black, acicular to elongated, bladed (ruler-shaped) and prismatic crystals (Fig. 1), which are found as individual crystals but more typically as radiating sprays and hemispherical aggregates. The maximum length of crystals is 0.5 mm and hemispherical aggregates can reach up to ~3 mm across. Crystals are elongated along [001] and the principal forms observed are {100} (the dominant platy face) and small {010} and {001} (*Bbmm* setting, see below).

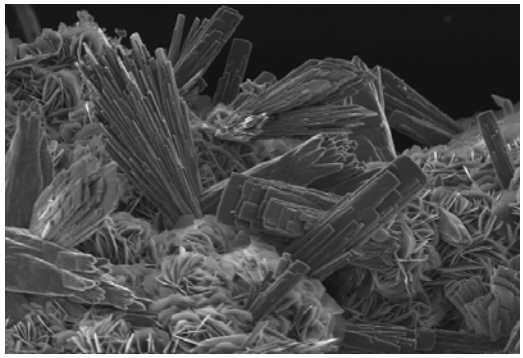

FIG. 1. SEM image showing sprays of bladed crystals of plimerite on hinsdalite-plumbogummite. The crystals are elongated along [001] and flattened on (100), and show the principal form {100} and minor {010} and {001}. The horizontal field of view is ~0.3 mm and the largest crystals are ~0.1 mm long.

Plimerite is translucent with a pale-greyish-green streak and a vitreous lustre. It shows an excellent cleavage parallel to {100} and {010} and distinct cleavage parallel to {001}. It is brittle, has an uneven fracture, a Mohs' hardness of 3.5 to 4, a measured density (sink-float method using Clerici solution-water mixture) of 3.67(5) g/cm^3 and a calculated density of 3.62 g/cm^3 (for the empirical formula). It shows no observable fluorescence under ultraviolet light. Optically, plimerite is biaxial negative with α = 1.756(5), β = 1.764(4), γ = 1.767(4). The optic angle could not be measured but it is large, and $2V$(calc.) is −63º. The optical orientation is XYZ = *cab* and the pleochroism is X pale-greenish-brown, Y pale-brown, Z pale-bluish-green, with absorption Z > X > Y. A Gladstone-Dale calculation gave a compatibility index of 0.10, poor (Mandarino, 1981). The reason for the poor compatibility is thought to be due the strong influences of the clearly variable chemical composition of individual crystals (Zn:Fe and Fe^{2+}:Fe^{3+} ratios) on the optical properties.

Chemical analysis

Grains from several specimens of plimerite-rockbridgeite were mounted in an epoxy block, polished, carbon coated and analysed using a CAMECA SX51 electron microprobe operating in the wavelength dispersion mode, with an accelerating voltage of 20 kV, a probe current of 20 nA and a probe diameter of 20 μm. Data were reduced using the $\phi(\rho Z)$ method of Pouchou and Pichoir (1985). The following standards and X-ray lines were used for the analyses: crocoite for Pb-$M\alpha$; hydroxylapatite for Ca-$K\alpha$ and P-$K\alpha$; sphalerite for Zn-$K\alpha$; rhodonite for Mn-$K\alpha$; almandine for Mg-$K\alpha$, Fe-$K\alpha$ and Al-$K\alpha$; and arsenopyrite for As-$K\alpha$.

The totals of the analyses are slightly low after inclusion of the theoretical water content from the structure determination (range: 97.30 to 97.89 wt.%, Table 2). The reason is unclear. Elements detected in amounts <0.05 wt.% were Mg, Mn, Cu, Si, S and K, while elements sought but not detected were Na, Cl, Cr, Ni, Sr, Sb and Ba. As a check, the standards, and several other phosphate and arsenate minerals, including two rockbridgeites, were analysed and all analytical totals were satisfactory. Moore (1970) noted that analysed rockbridgeites consistently show a slightly larger than ideal water content, probably reflecting the fibrous habit of the material, which may permit the presence of some occluded water. The analyses of Sejkora *et al*. (2006*b*) were also characterized by low totals (94−97%), which were attributed to the possible presence of additional water molecules. An IR spectrum of plimerite from Broken Hill (Fig. 2) does not however indicate the presence of any molecular water.

Analytical results show that ZnO contents of rockbridgeite-plimerite from Broken Hill vary from 2.81−20.19 wt.%, with Al_2O_3 contents up to ~4.8 wt.% and As_2O_5 contents up to ~4.7 wt.%. The largest Zn content obtained was for a section of the crystal from the type specimen, used for single-crystal X-ray data collection (sample G32005) (Table 2).

The unit formula for the type specimen, calculated on the basis of 17 oxygens, is $Fe^{3+}_{2.53}Zn_{1.68}Al_{0.60}Fe^{2+}_{0.28}Ca_{0.02}Pb_{0.01}P_{3.09}As_{0.01}O_{17.00}H_{5.15}$, with the FeO and Fe_2O_3 contents estimated from the Mössbauer spectrum (see below) and water content calculated from the ideal formula from the crystal-structure solution. The end-member formula for plimerite is $ZnFe^{3+}_4(PO_4)_3(OH)_5$, which requires: ZnO 12.35, Fe_2O_3 48.49, P_2O_5 32.32, H_2O 6.84, total 100.00 wt.%.

Raman and infrared spectroscopy

Raman spectra of crystals of plimerite were recorded in the range from 4000 to 200 cm^{-1} with a Renishaw M1000 confocal micro-Raman

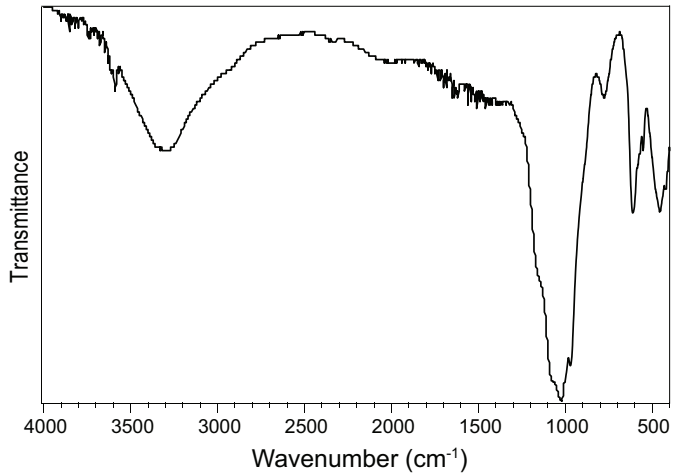

FIG. 2. FT-IR spectrum of powdered plimerite.

Imaging System using a 17 mW HeNe-laser at 632.8 nm and excitation through a Leica DMLM optical microscope (50 × /0.75 N.A. objective, 180º backscatter geometry, 1200 lines/mm grating, spectral resolution (apparatus function) 4 cm^{-1}, minimum lateral resolution ~2 μm, thermo-electrically-cooled CCD detector, random sample orientation). A representative spectrum (Fig. 3) shows bands due to OH stretching vibrations (at 3585 and a broad band ~3050 to ~3460 cm^{-1}, centred on 3300 cm^{-1}), ν_1 and ν_3 vibrations of the PO_4 tetrahedra (at 1110, 1055, 1018 and 965 cm^{-1}) and overlapping bands of the ν_4 and ν_2 vibrations of the PO_4 tetrahedra, vibrations of the $Fe(O,OH)_6$ and $(Zn,Fe)(O,OH)_6$ octahedra and lattice modes (at 631, 584, 474, 390, 297 cm^{-1}).

An infrared absorption spectrum of plimerite (Fig. 2) was recorded between 4000 and 400 cm^{-1} using a Nicolet Avatar 370Dtgs spectrometer and the CsI pressed-disk technique. A strong broad absorption band between 3720 and 2910 cm^{-1} (centred at about 3300 cm^{-1}) is attributed to OH stretching vibrations. The strong absorption bands at 1020 and 1060 cm^{-1} are attributed to ν_3 antisymmetric stretching modes of the PO_4 tetrahedra, the band at 966 cm^{-1} is a

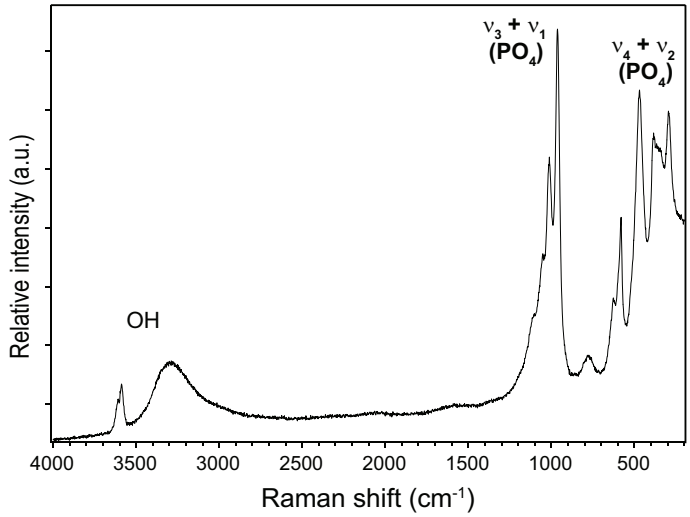

FIG. 3. Single-crystal Raman spectrum of plimerite (G32005).

symmetric stretching ν_1 mode of the PO_4 tetrahedra and the bands at 550 and 450 cm^{-1} are due to ν_4 and ν_2 bending modes of the PO_4 tetrahedra.

Mössbauer spectroscopy

Plimerite was gently ground in an agate mortar with acetone to make a powder which was mixed with benzophenone to avoid preferred orientation and loaded into a plexiglass sample holder with a 12 mm diameter. The Mössbauer thickness of the plimerite sample was determined from the chemical composition and the sample weight to be 5 mg Fe/cm^2. The Mössbauer spectrum was recorded at room temperature (293 K) in transmission mode on a constant acceleration Mössbauer spectrometer with a nominal 1.85 GBq ^{57}Co source in a 6 μm Rh matrix. The velocity scale was calibrated relative to a 25 μm thick α-Fe foil using the positions certified for (former) National Bureau of Standards standard reference material no. 1541; line-widths of 0.28 mm/s for the outer lines of α-Fe were obtained at room temperature. The spectrum was collected for one day, and was fitted using the commercially available fitting program *NORMOS* written by R.A. Brand (distributed by Wissenschaftliche Elektronik GmbH, Germany).

The Mössbauer spectrum (Fig. 4) is dominated by a single quadrupole doublet, but contains additional absorption indicating the presence of a minor amount of additional components. Initially, we fitted the spectrum with three Lorentzian doublets, but the residual was extremely large. A significantly better fit was obtained with three Voigt doublets according to the Voigt-based method for line-shape analysis (Rancourt and Ping, 1991) with the Lorentzian linewidth of the Voigt line-shape constrained to be equal for all doublets. Conventional constraints were applied to the components of each doublet (i.e., equal area, equal line-shape and equal linewidth). The hyperfine parameters are summarized in Table 3.

One doublet (having a larger centre shift and quadrupole splitting) was assigned to Fe^{2+} and two doublets (having a smaller centre shift and quadrupole splitting) were assigned to Fe^{3+} with different environments, although this does not imply that Fe^{3+} occupies (only) two sites in the structure. The centre shifts are consistent with octahedral coordination corresponding to each of the three doublets. The assignment is also in accord with the tendency for ferric Fe in octahedral sites to display higher quadrupole splitting with greater octahedral distortion (e.g. Bancroft *et al*., 1967).

The relative areas show that 89% of Fe occurs as Fe^{3+}, and the relative area fraction of the two

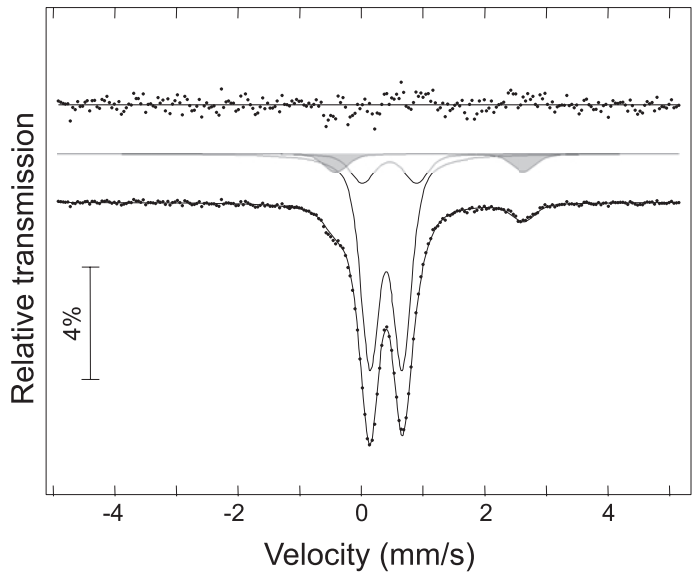

FIG. 4. Mössbauer spectrum of plimerite at room temperature. Doublets are shaded as follows: Fe^{3+} (unshaded); Fe^{2+} (grey). The residual (difference between experimental data and calculated curve) is shown above the spectrum, and the velocity scale is calibrated relative to α-Fe.

TABLE 3. ^{57}Fe Mössbauer hyperfine parameters for plimerite at room temperature.

	$^{I}Fe^{3+}$	$^{II}Fe^{3+}$	Fe^{2+}
Centre shift (mm/s)[a]	0.40(1)	0.38(2)	1.10(2)
Quadrupole splitting (mm/s)	0.35(1)	0.92(2)	3.44(2)
Gaussian sigma (mm/s)	0.06(1)	0.10(1)	0.05(1)
Lorentzian FWHM (mm/s)[b]	0.24(1)	0.24(1)	0.24(1)
Area fraction	0.62(2)	0.27(2)	0.11(2)

[a] relative to α-Fe
[b] constrained to be equal for each component.

Fe^{3+} components is approximately 2:1, which in good agreement with the expected occupancy of the *M*(3) and *M*(1) sites in the structure by Fe derived from chemical analysis and structure determination. We therefore assign the doublets as follows: $^{I}Fe^{3+}$ (low QS) – *M*(3); $^{II}Fe^{3+}$ (high QS) – *M*(1).

Two studies of rockbridgeite using Mössbauer spectroscopy have been completed (Amthauer and Rossman, 1984; Redhammer *et al*., 2006). Both of these groups fitted their spectra with four doublets, two assigned to Fe^{3+} and two assigned to Fe^{2+}, but there were differences in the assignment of the doublets. Amthauer and Rossman (1984) assigned the Fe^{3+} doublet with the smaller QS to the Fe(1) site and that with larger QS to the Fe(3) site based on the area ratios, although they noted that the results did not fully agree with the structure refinement. They assigned a low intensity Fe^{3+} doublet to the Fe(2) site, and the Fe^{2+} doublets with high and low QS were assigned to the Fe(2) and Fe(3) sites, respectively. However, Redhammer *et al*. (2006), on the basis of their structural data which showed that both the Fe(1) and Fe(3) sites are occupied by only Fe^{3+}, assigned the Fe^{3+} doublet with the smaller QS to the Fe(3) site and the Fe^{3+} doublet with the larger QS to the Fe(1) site, consistent with our assignments.

XRD data

Powder XRD data for plimerite (Table 4) were obtained using a Guinier-Hägg camera, 100 mm in diameter, and Cr-*K*α radiation (λ = 2.28970 Å). Silicon powder (NBS SRM 640a) was used as an internal standard. The unit-cell parameters were refined by treating the whole powder pattern with the Le Bail profile-fitting method (Le Bail *et al*., 1988), starting from the unit-cell parameters determined using single-crystal techniques. The final unit-cell parameters, a = 13.804(4) Å, b = 16.736(4) Å, c = 5.145(5) Å, V = 1188.6(6) Å^3, are very similar to those obtained from refinement using single-crystal methods. The axial ratios calculated from these cell parameters are 0.8248:1:0.3074.

Single-crystal XRD

Single-crystal X-ray data were collected using two crystals from different specimens of plimerite. Many crystals were examined using a polarizing microscope, however none were found that were not in sub-parallel intergrowth with other smaller individuals. A crystal from the type specimen (South Australian Museum specimen G32005) was cleaved on (010) into several fragments. Data were collected at room temperature, using the fragment (0.11 mm × 0.02 mm × 0.016 mm in size) considered most suitable, with a Bruker APEX II KappaCCD diffractometer. The data were processed with *Apex2* software. Intensity data using a second crystal (South Australian Museum specimen G32401) were collected at room temperature using a Nonius KappaCCD single-crystal X-ray diffractometer. The data were processed with the Nonius program suite *DENZO-SMN*. All data were corrected for Lorentz, polarization, background and absorption effects (Otwinowski and Minor, 1997; Otwinowski *et al*., 2003). Conditions for the data collection and subsequent refinement are summarized in Table 5.

In both cases, the systematic absences pointed to the non-centrosymmetric space groups $Cmc2_1$and *Ama*2 and the centrosymmetric space group *Cmcm*, but the intensity statistics did not provide a conclusive indication of the presence of a centre of symmetry. The space group *Cmcm* was

TABLE 4. X-ray powder diffraction data for plimerite.

I_{obs}	d_{obs}	I_{calc}	d_{calc}	h	k	l	I_{obs}	d_{obs}	I_{calc}	d_{calc}	h	k	l
5	8.599	21	8.399	0	0	2			3	2.196	2	0	4
30	6.922	3	6.933	0	2	0	10	2.166	1	2.171	1	3	6
5	6.391	4	6.408	0	2	1	25	2.143	4	2.149	1	1	7
5	4.827	11	4.829	1	1	0			2	2.136	0	6	3
50	4.638	8	4.641	1	1	1	10	2.104	4	2.111	1	5	4
5	4.343	6	4.356	0	2	3			1	2.100	0	0	8
15	4.194	100	4.200	0	0	4	10	2.092	9	2.093	2	2	4
		3	4.186	1	1	2	20	2.049	13	2.052	2	4	1
35	3.651	3	3.657	1	1	3	10	2.014	3	2.010	0	2	8
30	3.579	28	3.592	0	2	4			1	1.973	0	4	7
35	3.433	20	3.466	0	4	0	40	1.957	26	1.961	2	2	5
		27	3.440	1	3	0	5	1.938	9	1.939	2	4	3
50	3.388	91	3.395	0	4	1	20	1.893	4	1.896	2	0	6
55	3.369	11	3.370	1	3	1	5	1.842	6	1.849	1	7	0
10	3.198	9	3.204	0	4	2	20	1.826	9	1.828	2	2	6
100	3.168	21	3.183	1	3	2			1	1.802	0	2	9
		9	3.169	1	1	4	5	1.793	2	1.796	0	4	8
10	3.017	53	3.023	0	2	5			1	1.782	0	6	6
5	2.936	19	2.947	0	4	3			1	1.756	1	7	3
10	2.794	10	2.800	0	0	6			27	1.733	0	8	0
60	2.753	12	2.758	1	1	5	5	1.729	3	1.724	0	8	1
5	2.667	3	2.673	0	4	4			4	1.720	2	6	0
		1	2.661	1	3	4			4	1.712	1	5	7
90	2.575	1	2.576	2	0	0			1	1.711	2	6	1
75	2.414	5	2.422	1	1	6	10	1.704	2	1.704	3	1	0
		5	2.416	1	5	1			1	1.697	0	8	2
		5	2.414	2	2	0			1	1.692	1	7	4
		6	2.412	0	4	5	10	1.681	8	1.685	2	6	2
50	2.400	10	2.404	1	3	5	10	1.677	28	1.680	0	0	10
		8	2.390	2	2	1				1.656	0	8	3
5	2.317	4	2.320	2	2	2	15	1.643	14	1.643	0	4	9
15	2.263	14	2.268	0	6	1			1	1.630	3	1	3
5	2.213	1	2.217	2	2	3			1	1.627	2	1	8

Observed intensities estimated visually.
Calculated intensities were obtained using the program *LAZY PULVERIX* (Yvon *et al*., 1977).

verified by successful solution and refinement of the structure. In order to facilitate comparison to rockbridgeite and frondelite, the setting of the space group was changed to the non-standard *Bbmm* at the final stage of the structure refinement.

The refined unit cell of plimerite is smaller than those of rockbridgeite and fondelite (Table 1), the volume of cells being 2.7% smaller for G32005 and 1.7% smaller for G32401 than the rockbridgeite of Redhammer *et al*. (2006). This is in accord with the smaller ionic radius of the Zn^{2+} ion (0.74 Å) compared to that of the Fe^{2+} ion (0.78 Å) (Shannon, 1976). The smaller cell for G32005 relative to G32401 (Table 5) also reflects increased Zn and Al contents. The cell of Moore (1970) is significantly smaller than that of Redhammer *et al*. (2006), possibly reflecting a higher degree of Fe oxidation.

Structure solution and refinement

All calculations were performed with the *SHELX* package of programs (Sheldrick, 1997*a*,*b*).

Complex scattering factors for neutral atoms were taken from the *International Tables for Crystallography* (Wilson, 1992). Solution of the structure using direct methods located the

TABLE 5. Crystal data, data collection and refinement details for plimerite.

	G32005	G32401
Crystal data		
Formula	$Zn_{1.41}Fe^{2+}_{0.30}Fe^{3+}_{2.71}Al_{0.58}(PO_4)_3(OH)_5$	$Zn_{1.17}Fe^{2+}_{0.37}Fe^{3+}_{3.46}PO_4)_3(OH)_5$
Space group	*Bbmm*	*Bbmm*
a (Å)	13.811(3)	13.865(3)
b (Å)	16.718(3)	16.798(3)
c (Å)	5.141(10)	5.151(10)
V (Å^3)	1187.0(4)	1199.7(4)
Z	4	4
F(000)	1207.9	1237.0
μ (mm^{-1})	6.55	6.75
Absorption correction	multi-scan	multi-scan
Crystal dimensions (mm)	0.11 x 0.02 x 0.016	0.29 x 0.03 x 0.03
Data collection		
Diffractometer	Bruker APEX II KappaCCD	Nonius KappaCCD
Temperature (K)	293	293
Radiation	Mo-*K*α, λ = 0.71073 Å	Mo-*K*α, λ = 0.71073 Å
Crystal detector distance (mm)	30	30*
Rotation axis, width (º)	φ, ω, 2.0	ϕ, ω, 1.5*
Total number of frames	448	~500*
Collection time per degree (s)	500	~250*
θ range (º)	2.44−28.36	2.42−36.53
h,*k*,*l* ranges	−6 → +6, −18 → +18, −22 → +22	−8 → +8, −23 → +22, −28 → +28
Total reflections measured	9305	8562
Data completeness	92.8%	96.3%
Unique reflections	790 (R_{int} = 0.0503)	1595 (R_{int} = 0.0527)
Refinement		
Refinement on	F^2	F^2
$R1^{\dagger}$ for $F_o > 4\sigma(F_o)$.	9.64%	6.41%
$wR2^{\ddagger}$ for all F_o^2	19.87%	14.57%
Reflections used $F_o^2 > 4\sigma(F_o^2)$	735	1332
Number of parameters refined	86	86
Extinction coefficient	0.0033(11)	0.0032(7)
Goodness of Fit	1.095	1.114
Δ/σ_{max}	0.000	0.000
$\Delta\rho_{max}$, $\Delta\rho_{min}$ (e/Å^3)	2.607, −2.705	1.480, −1.700

* Probable values (accurate measurement parameters lost due to computer crash)

† $R1 = \Sigma||F_o| - |F_c||/\Sigma|F_o|$

‡ $wR2 = \Sigma w(|F_o|^2 - |F_c|^2)^2/\Sigma w|F_o|^2)^{1/2}$; $w = 1/[\sigma^2(F_o^2) + (0.042\ P)^2 + 12.60\ P]$; P = ([max of (0 or F_0^2)] + $2F_c^2$)/3

positions of all cations, and refinement by a combination of least-squares refinement and difference-Fourier synthesis located the positions of eight O atoms. The positions of the H atoms could not be located in difference Fourier maps. Approximately 50 of the most disagreeable reflections, with F_{obs} considerably larger than F_{calc}, whose measured intensities had been most strongly affected by the poor quality of the crystal, were omitted. Refinement of the final model gave $R1$ = 9.64 %, $wR2$ = 20.07% for all 735 data $F_0 > 4\sigma(F_0)$ for G32005. A higher-quality refinement resulted for G32401 with $R1$ = 6.41 %, $wR2$ = 14.57% for all 1332 data $F_0 > 4\sigma(F_0)$ and details of this refinement are reported below. Refined coordinates and anisotropic-displacement factors are listed in Table 6, selected bond lengths and angles and possible hydrogen bonds (Brown and Altermatt, 1985) are given in Table 7. Large values of the reliability

TABLE 6. Fractional coordinates and displacement parameters (Å^2) of atoms for plimerite (G32401).

	x	y	z	U_{eq}	U_{11}	U_{22}	U_{33}	U_{12}	U_{13}	U_{23}
$M(1)$*	0	0.5	0	0.0091(2)	0.0095(5)	0.0074(4)	0.0103(5)	0	0	−0.0004(4)
$M(2)$*	0.06888(6)	0.65849(5)	0	0.0168(2)	0.0158(4)	0.0086(3)	0.0259(4)	0	0	−0.0005(3)
$M(3)$*	0.32193(8)	0.63906(6)	0.2323(2)	0.0087(2)	0.0095(4)	0.0068(4)	0.0097(4)	0.0001(4)	0.0014(4)	−0.0007(3)
P(1)	0.14325(10)	0.54388(8)	0.5	0.0096(3)	0.0091(6)	0.0056(5)	0.0141(6)	0	0	−0.0004(4)
P(2)	0.48312(15)	0.75	0	0.0120(4)	0.0112(9)	0.0072(7)	0.0176(9)	0	0	0
O(1)	0.5464(4)	0.75	−0.2479(11)	0.0201(9)	0.020(2)	0.0146(18)	0.025(2)	0	0.0123(19)	0
O(2)	0.0811(2)	0.55837(18)	0.2562(6)	0.0151(5)	0.0146(13)	0.0189(13)	0.0117(12)	0.0004(11)	−0.0038(10)	−0.0050(10)
OH(3)	0.3147(6)	0.75	0.3801(17)	0.0144(15)	0.019(4)	0.008(3)	0.016(4)	0	0.008(3)	0
O(4)	0.1813(4)	0.4595(3)	0.5	0.0278(12)	0.019(2)	0.0082(17)	0.056(4)	0	0	0.0042(16)
OH(5)	0.2154(3)	0.6745(3)	0	0.0198(9)	0.0139(19)	0.0099(17)	0.036(3)	0	0	0.0025(15)
OH(6)	0.0749(3)	0.3947(3)	0	0.0137(7)	0.0131(18)	0.0151(18)	0.0131(17)	0	0	0.0034(15)
O(7)	0.4211(3)	0.6745(3)	0	0.0160(8)	0.017(2)	0.0096(16)	0.021(2)	0	0	−0.0043(14)
O(8)	0.2238(3)	0.6063(3)	0.5	0.0126(7)	0.0123(17)	0.0105(16)	0.0150(18)	0	0	−0.0020(13)

The anisotropic displacement parameters (U_{ij}) are defined as $\exp[-2\pi^2\Sigma_{i=}^{3}\Sigma_{\varphi=1}3jU_{ij}a_i^*\ a_j^*\ h_ih_j]$

* Refined occupancies: $M1 = Fe_{0.99}$; $M2 = Zn_{0.58}Fe_{0.42}$; $M3 = Fe_{0.94}Al_{0.06}$.

TABLE 7. Selected interatomic distances (Å), angles (°) and suggested hydrogen-bonds for plimerite (G32401).

M(1)	O(2) ×4	1.991(3)	P(1)	O(4)	1.512(5)
	OH(6) ×2	2.050(4)		O8	1.532(4)
	<*M*(1)–O>	2.011		O(2) ×2	1.543(3)
				<P(1)–O>	1.533
M(2)	O(1) ×2	2.036(4)			
	OH(5)	2.049(5)	P(2)	O(7) ×2	1.532(4)
	O(2) ×2	2.144(3)		O(1) ×2	1.549(5)
	OH(6)	2.184(4)		<P(1)–O>	1.541
	<*M*(2)–O>	2.099			
M(3)	O(7)	1.917(4)			
	OH(5)	1.992(4)			
	OH(3)	2.013(3)			
	O8	2.016(3)			
	O(4)	2.043(4)			
	OH(6)	2.067(3)			
	<*M*(3)–O>	2.008			

O(7)–P(1)–O(7)	111.5(4)	O(4)–P(2)–O8	112.8(3)
O(7)–P(1)–O(1) ×4	108.57(13)	O(4)–P(2)–O(2) ×2	110.06(16)
O(1)–P(1)–O(1)	111.0(4)	O8–P(2)–O(2) ×2	107.44(15)
<O(1)–P(1)–O(1)>	109.46	O(2)–P(2)–O(2)	109.0(3)
		<O(2)–P(2)–O(2)>	109.47

Atomic separations corresponding to possible hydrogen-bonds*.

OH(5)–OH(5)	2.534

* All other O···O distances > 3.2 Å are along polyhedra edges.

factors are characteristic of Fe-bearing phosphate minerals due to the typical small size and fibrous nature of the crystals.

No hydrogen atoms were detected in the difference Fourier map and the concept of bond-valences (Brese and O'Keeffe, 1991; Brown, 1996) was used to identify the hydroxyl groups (Table 8).

Crystal-structure description

Cation sites

The structure of plimerite contains three *M* sites, each surrounded by six anions in a distorted octahedral coordination with *M*–ϕ [ϕ: O^{2-}, OH] distances ranging from 1.917 to 2.184 Å, values that are typical for octahedra involving medium-sized trivalent and divalent cations.

The observed mean *M*(1)–ϕ bond length of 2.011 Å is in accord with the calculated <*M*–ϕ> distance of 2.005 Å (Shannon, 1976) for complete occupancy of the *M*(1) site by Fe^{3+}. The occupancy factor of 0.991(2) from site-occupancy refinement and the bond-valence sum of 3.04 valence units (v.u.) (Table 8) also both support the occupancy of the *M*(1) site by predominantly Fe^{3+}.

The bond-valence sum for the *M*(2) site (1.98 v.u.) agrees with the occupancy of the position by predominantly divalent cations. The observed <*M*–ϕ> distance is 2.099 Å which compares to a value of 2.084 Å for an occupancy of $(Zn_{1.20}Fe^{2+}_{0.38}Fe^{3+}_{0.42})$ calculated from the chemical analysis (Table 2). A refinement of the Zn:Fe occupancy gave a ratio of 0.581(3):419 which is in reasonably good agreement with the site occupancy from the chemical analysis.

The bond-valence sum for the *M*(3) site (3.07 v.u.) and the observed <*M*–ϕ> distance of 2.008 Å agrees with occupancy of the site by

TABLE 8. Bond valence* (v.u.) table for plimerite.

	M(1)	*M*(2)	*M*(3)	P(1)	P(2)	Sum
O(1)		$0.43^{\times 2}\downarrow\rightarrow$			$1.20^{\times 2}$	2.06
O(2)	$0.53^{\times 4}\downarrow$	$0.32^{\times 2}\downarrow$		$1.22^{\times 2}\downarrow$		2.07
OH(3)			$0.50^{\times 2}\rightarrow$			1.00
O(4)			0.46	1.33		1.79
OH(5)		0.41	0.53			0.94
OH(6)	$0.46^{\times 2}\downarrow$	0.29	0.43			1.18
O(7)			0.65		$1.26^{\times 2}$	1.91
O(8)			0.50	1.26		1.76
Sum	3.04	2.20	3.07	5.03	4.92	

* Bond-valence parameters used are from Brese and O'Keeffe (1991).
Bond valences for the *M*(2) site are based an occupancy of $(Zn_{1.20}Fe^{2+}_{0.38}Fe^{3+}_{0.42})$.

predominantly Fe^{3+}. The <*M*−ϕ> distance of 1.988 Å for the *M*(3) site for G32005, which contains 0.58 a.p.f.u. Al, suggests that a significant percentage of the Al is located at this site. The distances between *M*(3) sites along the *c* direction are alternately 2.394 and 2.758 Å and full occupancy of the site would result in infinite chains, consisting of edge-sharing pairs of face-sharing octahedra. Due to repulsive forces, a short Fe−Fe interatomic distance of 2.394 Å across shared octahedra faces is highly improbable, hence only alternate *M*(3) sites can be considered to be simultaneously occupied. The refined occupancy of the *M*(3) site is 0.486(5). Half-occupancy of this site also agrees with the stoichiometry derived from the chemical analysis (Table 2), which requires 20 Fe atoms in the unit cell, as opposed to 28 if the site was fully occupied. Half occupancy of the site also agrees with the results of Moore (1970) and Redhammer *et al*. (2006) for rockbridgeite. Partial occupancy of equivalent Fe sites has been documented in the crystal structures of lipscombite, $Fe^{2+}Fe^{3+}_2(OH)_2(PO_4)_2$ (Katz and Lipscomb, 1951, Vencato *et al*., 1989), where full occupancy would result in infinite face-sharing octahedral columns, whitmoreite (Moore *et al*., 1974), 'laubmannite' (Kolitsch, 2004) and synthetic $Fe^{2+}Fe^{3+}_2(PO_3OH)_4(H_2O)_4$ (Vencato *et al*., 1986).

The structure of plimerite contains two P sites, each coordinated by four O atoms in a tetrahedral arrangement. The average <P(1)−O> and <P(2)−O> bond lengths are 1.541 Å and 1.533 Å respectively, which are in good agreement with the average <P−O> distance of 1.537 Å [range: 1.439−1.625 Å] for phosphate minerals (Baur, 1981; Huminicki and Hawthorne, 2002).

Anion sites

There are eight anion sites in the structure, each occupied by O atoms. The O(1), O(2), O(4), O(7) and O(8) anions each have an incident bond-valence sum of ~2.0 v.u. (Table 8) and are O^{2-} anions. The OH(3), OH(5) and OH(6) anions have incident bond-valence sums of ~1.0 v.u. and so must be (OH) groups. The OH(3) site is situated ~0.65 Å from a mirror plane, resulting in an OH(3)−OH(3) distance of ~1.31 Å, and thus the site is unlikely to be fully occupied. The refined occupancy of the site is ~50%, which is in agreement with the results of Moore (1970) and Redhammer *et al*. (2006) for rockbridgeite.

The formula of plimerite requires replacement of both divalent and trivalent Fe by Zn^{2+} in the rockbridgeite-frondelite general formula, $A^{2+}B^{3+}_4(TO_4)_3(OH)_5$, with a resulting deficit of positive charges. The O(4) and O(8) anions, which bond to *M*(3) and P(1) and do not accept any hydrogen bonds, are somewhat undersaturated, with bond-valence sums of 1.79 and 1.76 v.u. respectively. This suggests that these anions might represent a mixture of O^{2-} and OH^{-} which would provide the additional positive charges required to maintain electroneutrality of the formula.

Structure topology

The structure of plimerite is based on a trimer of face-sharing octahedra, the '*h*-cluster' described by Moore (1970). A central ($M1\phi_6$) octahedron

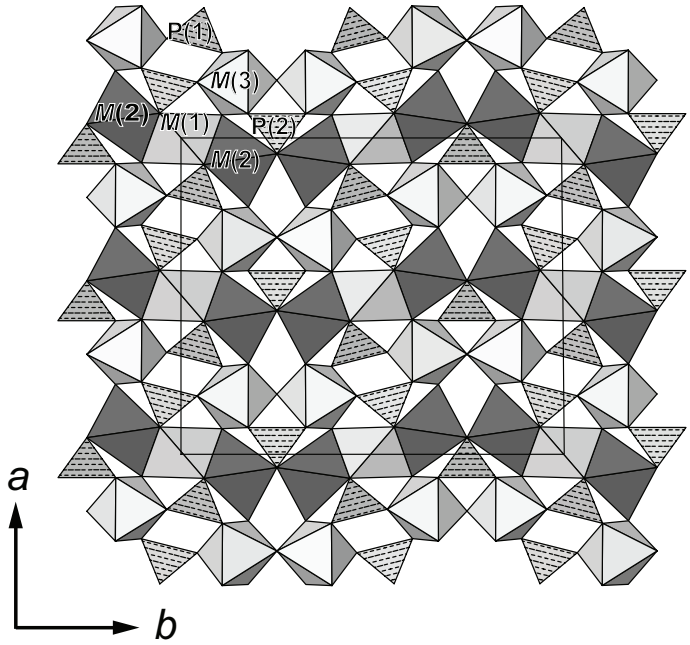

FIG. 5. The crystal structure of plimerite projected onto (001). The unit cell is outlined. All structure drawings were completed using *ATOMS* (Shape Software 1997).

shares two *trans* faces with ($M2\phi_6$) octahedra, through the O(2) and OH(6) anions, to form a trimer of the form [$M_3\phi_{12}$]. The face-sharing trimers link by sharing octahedron edges to form chains of octahedra, that extend in the *b* direction (Fig. 5). ($M3\phi_6$) octahedra link *via* corner sharing to form pairs of octahedra which then link to corners of PO_4 tetrahedra forming [$M_2(TO_4)\phi_8$] clusters. Chains of octahedra adjacent in the *a* direction are linked by [$M_2(TO_4)\phi_8$] clusters and PO_4 groups that link to adjacent trimers and two [$M_2(TO_4)\phi_8$] clusters, forming complex sheets parallel to (001). The structure can be classified as a heteropolyhedral framework but with a distinct layered nature (Fig. 6), with layers of octahedra, parallel to (001), alternating with layers of tetrahedra.

Related structures

Trimers of face-sharing octahedra ('*h*-clusters') are a feature of the structures of a number of basic Fe-phosphate minerals, among them the isostructural minerals dufrénite, $Ca_{0.5}Fe^{2+}Fe^{3+}_5(PO_4)_4(OH)_6(H_2O)_2$ (Moore, 1970), burangaite, $Na[Fe^{2+}Al_5(PO_4)_4(OH)_6(H_2O)_2]$ (Selway *et al*., 1997) and matioliite, $NaMgAl_5(PO4)_4(OH)_6{\cdot}2H_2O$ (Atencio *et al*., 2006); the minerals of the lazulite group, lazulite, $MgAl_2(PO_4)_2(OH)_2$ (Guiseppetti and Tadini, 1983), scorzalite, $(Fe^{2+},Mg)Al_2(PO_4)_2(OH)_2$ (Lindberg and Christ, 1959); the isostructural minerals barbosalite, $Fe^{2+}Fe^{3+}_2(PO_4)_2(OH)_2$ (Redhammer *et al*., 2000) and hentschelite, $CuFe^{3+}_2(PO_4)_2(OH)_2$, (Sieber *et al*., 1987); as well as beraunite, $Fe^{2+}Fe^{3+}_5(PO_4)_4(OH)_5{\cdot}6H_2O$ (Moore and Kampf, 1992) and souzalite/gormanite, $(Fe,Mg)_3(Al,Fe)_4(PO_4)_4(OH)_6{\cdot}2H_2O$ (Le Bail *et al*., 2003). The different modes of linkage of the clusters yield several different structure types.

In the lazulite-group minerals, adjacent trimers of octahedra, which run parallel to [110] and [$\bar{1}$10], link by sharing corners with PO_4 groups forming layers of octahedra and tetrahedra parallel to (100), which then link forming a dense framework. The trimers have the form $Al^{3+} = Mg^{2+} = Al^{3+}$ for lazulite, $Al^{3+} = Fe^{2+} = Al^{3+}$ for scorzalite, $Fe^{3+} = Fe^{2+} = Fe^{3+}$ for barbosalite and $Fe^{3+} = Cu = Fe^{3+}$ for hentschelite.

In the structures of the dufrénite-group minerals the face-sharing triplet of octahedra are

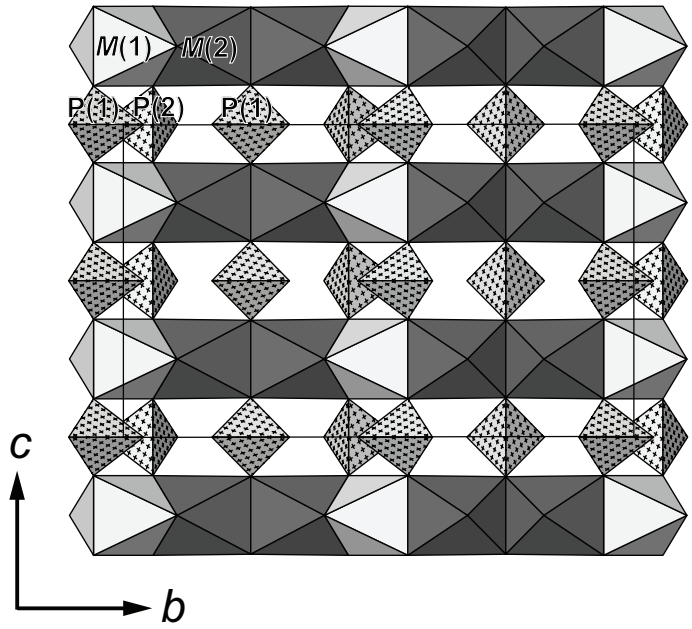

FIG. 6. The crystal structure of plimerite projected onto (100). The unit cell is outlined.

corner-linked to two $M\phi_6$ octahedra and two PO_4 tetrahedra to form a $[M_5(TO_4)_2\phi_{18}]$ cluster which is polymerized parallel to the *c* axis to form dense slabs in the {100} plane. The slabs link in the [100] direction by sharing corners, with an additional $M\phi_6$ octahedron. In dufrénite trimers of face-sharing octahedra have the form $Fe^{3+} \equiv Fe^{2+} \equiv Fe^{3+}$, in burangaite, $Al^{3+} \equiv Fe^{2+} \equiv Al^{3+}$ and in matioliite, $Al^{3+} \equiv Mg \equiv Al^{3+}$.

In souzalite the face-sharing trimers differ in that they have the form $M^{2+} \equiv M^{3+} \equiv M^{2+}$ with the central octahedron being that of the trivalent cation. Trimers share edges with $Fe\phi_6$ octahedra to form $\cdots = Fe^{3+} = Mg \equiv Al \equiv Mg = \cdots$ infinite chains that run along [010]. Chains link, in the [101] direction, *via* corners to two additional symmetrically distinct $Al\phi_6$ octahedra to form sheets in the {100} plane which then link in the [001] direction to an adjacent sheet *via* PO_4 groups.

In the beraunite structure face-sharing trimers are corner-linked to $Fe\phi_6$ octahedra to form chains parallel to [001]. The chains link to PO_4 groups forming thick sheets in the (100) plane which link *via* $Fe\phi_6$ octahedra into a framework. Channels along [010] are occupied by H_2O molecules.

Chains of face-sharing octahedra, which closely resemble the '*h*-cluster', are found in the structure of lipscombite (Vencato *et al*., 1989; Yakubovich *et al*., 2006).

Acknowledgements

The authors thank the staff of Adelaide Microscopy, The University of Adelaide, especially Angus Netting for assistance with the electron microprobe analysis and the SEM photomicrograph. Christine Ta provided assistance with collecting the infrared spectra of plimerite. We thank Fernando Cámara, Günther Redhammer and Principal Editor Mark Welch for their comments on this paper.

References

Amthauer, G. and Rossman, G.R. (1984) Mixed valence of iron in minerals with cation clusters. *Physics and Chemistry of Minerals*, **11**, 37–51.

Atencio, D., Coutinho, J.M.V., Mascarenhas, Y.P. and Ellena, J.A. (2006) Matioliite, the Mg-analogue of burangaite, from Gentil mine, Mendes Pimentel, Minas Gerais, Brazil, and other occurrences. *American Mineralogist*, **91**, 1932–1936.

Bancroft, G.M., Maddock, A.G. and Burns, R.G. (1967) Applications of the Mössbauer effect to silicate mineralogy-I. Iron silicates of known crystal

structure. *Geochimica et Cosmochimica Acta*, **31**, 2219–2246.

Baur, W.H. (1981) Interatomic distance predictions for computer simulation of crystal structures. Pp. 31–52 in: *Structure and Bonding in Crystals II* (M. O'Keeffe and A. Navrotsky, editors). Academic Press, New York.

Birch, W.D. (1990) Minerals from the Kintore and Block 14 Opencuts, Broken Hill, N.S.W.; a review of recent discoveries, including tsumebite, kipushite and otavite. *Australian Mineralogist*, **5**, 125–141.

Birch, W.D. (1999) The Minerals. Pp. 88–256 in: *Minerals of Broken Hill* (W.D. Birch, editor). Broken Hill Council, Broken Hill, Australia.

Birch, W.D. and van der Heyden, A. (1988) Minerals of the Kintore Opencut, Broken Hill, New South Wales. *Mineralogical Record*, **19**, 425–436.

Birch, W.D. and van der Heyden, A. (1997) Minerals from the Kintore and Block 14 Open cuts, Broken Hill, New South Wales. *Australian Journal of Mineralogy*, **3**, 23–71.

Brese, N.E. and O'Keeffe, M. (1991) Bond-valence parameters for solids. *Acta Crystallographica B*, **47**, 192–197.

Brown, I.D. and Altermatt, D. (1985) Bond-valence parameters obtained from a systematic analysis of the inorganic crystal structure database. *Acta Crystallographica B*, **41**, 244–247.

Brown, I.D. (1996) *VALENCE*: a program for calculating bond-valences. *Journal of Applied Crystallography*, **29**, 479–480.

Campbell, J.L. (1881) On dufrenite from Rockbridgeite Co., Va. *American Journal of Science*, **22**, 65–67.

Frondel, C. (1949) The dufrenite problem. *American Mineralogist*, **34**, 513–540.

Ginzburg, A.I. (1952) The phosphates of granite pegmatites. Trudy Mineralogicheskogo Muzeya *Akademiya Nauk SSSR*, **4**, 36–63.

Guiseppetti, G. and Tadini, C. (1983) Lazulite, (Mg, Fe)$Al_2(OH)_2(PO_4)_2$: structure refinement and hydrogen bonding. *Neues Jahrbuch für Mineralogie Monatshefte*, 410–416.

Hirson, J.R. (1965) Nota sobre os fosfatos de Sapucaia. *Anais da Academia Brasileira de Ciências*, **37**, 471–475.

Huminicki, D.M.C. and Hawthorne, F.C. (2002) The crystal chemistry of the phosphate minerals. Pp. 123–253 in: *Phosphates: Geochemical, Geobiological, and Materials Importance* (M.J. Kohn, J. Rakovan and J.M. Hughes, editors). Reviews in Mineralogy and Geochemistry, **48**, Mineralogical Society of America, Chantilly, Virginia, USA.

Johnson, J.E. (1978) Zinc phosphate minerals from Reaphook Hill, South Australia. *Australian Mineralogist*, **1**, 65–68.

Katz, L. and Lipscomb, W.N. (1951) The crystal structure of iron lazulite, a synthetic mineral related to lazulite. *Acta Crystallographica*, **4**, 345–348.

Kolitsch, U. (2004) The crystal structures of kidwellite and 'laubmannite', two complex fibrous iron phosphates. *Mineralogical Magazine*, **68**, 147–165.

Le Bail, A., Duroy, H. and Fourquet, J.L. (1988) Ab-initio structure determination of $LiSbWO_6$ by X-ray powder diffraction. *Materials Research Bulletin*, **23**, 447–452.

Le Bail, A., Stephens. P.W. and Hubert, F. (2003) A crystal structure for the souzalite/gormanite series from synchrotron powder diffraction data. *European Journal of Mineralogy*, **15**, 719–723.

Lindberg, M.L. (1949) Frondelite and the frondelite-rockbridgeite series. *American Mineralogist*, **34**, 541–549.

Lindberg, M.L. and Frondel, C. (1950) Zincian rockbridgeite. *American Mineralogist*, **35**, 1028–1034.

Lindberg, M.L. and Christ, C.L. (1959) Crystal structures of the isostructural minerals lazulite, scorzalite and barbosalite. *Acta Crystallographica*, **12**, 695–697.

Mandarino, J.A. (1981) The Gladstone-Dale relationship: Part IV: The compatibility concept and its application. *The Canadian Mineralogist*, **19**, 441–450.

Massie, F.A. (1880) On the composition of dufrenite from Rockbridgeite Co., Va. *Chemical News*, **42**, 181.

Moore, P.B. (1969) The basic ferric phosphates: a crystallochemical principle. *Science*, **164**, 1063–1064.

Moore, P.B. (1970) Crystal chemistry of the basic iron phosphates. *American Mineralogist*, **55**, 135–169.

Moore, P.B. and Kampf, A.R. (1992) Beraunite: Refinement, comparative crystal chemistry, and selected bond valences. *Zeitschrift für Kristallographie*, **201**, 263–281.

Moore, P.B., Kampf, A.R. and Irving, A.J. (1974) Whitmoreite, $Fe^{2+}Fe_2^{3+}(OH)_2(H_2O)_4[PO_4]_2$, a new species: Its description and atomic arrangement. *American Mineralogist*, **59**, 900–905.

Otwinowski, Z. and Minor, W. (1997) Processing X-ray diffraction data collected in oscillation mode. Pp. 307–326 in: *Macromolecular Crystallography* (C.W. Carter, Jr. and R.M. Sweet, editors). Vol. **276**. Academic Press, New York.

Otwinowski, Z., Borek, D., Majewski, W. and Minor, W. (2003) Multiparametric scaling of diffraction intensities. *Acta Crystallographica A*, **59**, 228–234.

Pouchou, J.L. and Pichoir, F. (1985) 'PAP' $\phi(\rho Z)$ procedure for improved quantitative microanalysis. Pp. 104–106 in: *Microbeam Analysis* (J.T. Armstrong, editor). San Francisco Press, San Francisco, California, USA.

Redhammer, G.J., Tippelt, G., Roth, G., Lottermoser, W. and Amthauer, G. (2000) Structure and Mössbauer spectroscopy of barbosalite $Fe^{2+}Fe^{3+}_2(PO_4)_2(OH)_2$ between 80 K and 300 K. *Physics and Chemistry of Minerals*, **27**, 419–429.

Redhammer, G.J., Roth, G., Tippelt, G., Bernroider, M., Lottermoser, W., Amthauer, G. and Hochleitner, R. (2006) Manganoan rockbridgeite: structure analysis and ^{57}Fe Mössbauer spectroscopy. *Acta Crystallographica C*, **62**, i24–i28.

Rancourt, D.G. and Ping, J.Y. (1991) Voigt-based methods for arbitrary-shape static hyperfine parameter distributions in Mössbauer spectroscopy. *Nuclear Instruments and Methods in Physics Research B*, **58**, 85–97.

Sejkora, J., Škoda, R., Ondru, P., Beran, P. and Süsser, C. (2006*a*) Mineralogy of phosphate accumulations in the Huber stock, Krásno ore district, Slavkovsk les area, Czech Republic. *Journal of the Czech Geological Society*, **51**, 103–147.

Sejkora, J., Škoda, R. and Ondru, P. (2006*b*) New naturally occurring mineral phases from Krásno-Horní Slavkov area, western Bohemia, Czech republic. *Journal of the Czech Geological Society*, **51**, 159–187.

Selway, J.B., Cooper, M.A. and Hawthorne, F.C. (1997) Refinement of the crystal structure of burangaite. *The Canadian Mineralogist*, **35**, 1515–1522.

Shannon, R.D. (1976) Revised effective ionic radii and systematic studies of interatomic distances in halides and chalcogenides. *Acta Crystallographica A*, **32**, 751–767.

Shape Software (1997) *ATOMS* for Windows and Macintosh V 4.0, Kingsport, Tennessee, USA.

Sheldrick, G.M. (1997*a*) *SHELXS-97*, a Program for the Solution of Crystal Structures. University of Göttingen, Göttingen, Germany.

Sheldrick, G.M. (1997*b*) *SHELXL-97*, a Program for Crystal Structure Refinement. University of Göttingen, Göttingen, Germany.

Sieber, N.H.W., Tillmanns, E. and Hofmeister, W. (1987) Structure of hentschelite, $CuFe_2(PO_4)_2(OH)_2$, a new member of the lazulite group. *Acta Crystallographica C*, **43**, 1855–1857.

Vencato, I., Mascarenhas, Y.P. and Mattievich, E. (1986) The crystal structure of $Fe^{2+}Fe^{3+}_2(PO_3OH)_4(H_2O)_4$: a new synthetic compound of mineralogic interest. *American Mineralogist*, **71**, 222–226.

Vencato, I., Mattievich, E. and Mascarenhas, Y.P. (1989) Crystal structure of synthetic lipscombite: a redetermination. *American Mineralogist*, **74**, 456–460.

Willis, I.L., Brown, R.E., Stroud, W.J. and Stevens, B.P.J. (1983) The Early Proterozoic Willyama Supergroup: Stratigraphic sub-division and interpretation of high to low grade metamorphic rocks in the Broken Hill Block, N.S.W. *Journal of the Geological Society of Australia*, **30**, 195–224.

Wilson, A.I.C., editor. (1992) *International Tables for Crystallography*, **C**, 883 pp. Kluwer Academic, Dordrecht, The Netherlands.

Yakubovich, O.V., Steele I.M., Rusakov, V.S. and Urusov, V.S. (2006) Hole defects in the crystal structure of synthetic lipscombite $(Fe^{3+}_{4.7}Fe^{2+}_{2.3})[PO_4]_4O_{2.7}(OH)_{1.3}$ and genetic crystal chemistry of minerals of the lipscombite-barbosalite series. *Crystallography Reports*, **51**, 401–411.

Yvon, K., Jeitschko, W. and Parthé, Â.E. (1977) *LAZY PULVERIX*, a computer program, for calculating X-ray and neutron diffraction powder patterns. *Journal of Applied Crystallography*, **10**, 73–74.